Estimates of Near-Inertial Wind Power Input Using Novel In Situ Wind Measurements from Minimet Surface Drifters in the Iceland Basin

THILO KLENZ,[a] HARPER L. SIMMONS,[b] LUCA CENTURIONI,[c] JONATHAN M. LILLY,[d] JEFFREY J. EARLY,[e] AND VERENA HORMANN[c]

[a] *College of Fisheries and Ocean Sciences, University of Alaska Fairbanks, Fairbanks, Alaska*
[b] *Applied Physics Laboratory, University of Washington, Seattle, Washington*
[c] *Scripps Institution of Oceanography, La Jolla, California*
[d] *Planetary Science Institute, Tucson, Arizona*
[e] *NorthWest Research Associates, Redmond, Washington*

(Manuscript received 2 December 2021, in final form 8 June 2022)

ABSTRACT: The Minimet is a Lagrangian surface drifter measuring near-surface winds in situ. Ten Minimets were deployed in the Iceland Basin over the course of two field seasons in 2018 and 2019. We compared Minimet wind measurements to coincident ship winds from the R/V *Armstrong* meteorology package and to hourly ERA5 reanalysis winds and found that the Minimets accurately captured wind variability across a variety of time scales. Comparisons between the ship, Minimets, and ERA5 winds point to significant discrepancies between the in situ wind measurements and ERA5, with the most reasonable explanation being related to spatial offsets of small-scale storm structures in the reanalysis model. After a general assessment of the Minimet performance, we compare estimates of wind power input in the near-inertial band using the Minimet winds and their measured drift to those using ERA5 winds and the Minimet drift. Minimet-derived near-inertial wind power estimates exceed those from Minimet drift combined with ERA5 winds by about 42%. The results highlight the importance of accurately capturing small-scale, high-frequency wind events and suggest that in situ Minimet measurements are beneficial for accurately quantifying near-inertial wind work on the ocean.

SIGNIFICANCE STATEMENT: In this study we introduce a novel, freely drifting wind measurement platform, the Minimet. After an initial validation of Minimet sea surface wind measurements against independent wind measurements from a nearby research vessel, we investigate their utility in context of the near-inertial work done by the wind on the ocean, which is important for the ocean's energy budget. We find Minimet near-inertial wind work estimates exceed those estimated using winds from a state-of-the-art wind product by 42%. Our results indicate that capturing storm events happening on time scales less than 12 h is crucial for accurately quantifying near-inertial wind work on the ocean, making wind measurements from platforms such as the Minimet invaluable for these analyses.

KEYWORDS: Ocean; North Atlantic Ocean; Atmosphere-ocean interaction; In situ atmospheric observations; In situ oceanic observations; Wind profilers

1. Introduction

It has long been recognized that wind stress acting on the ocean surface accounts for a significant portion of the estimated 2 TW (Munk and Wunsch 1998; St. Laurent and Simmons 2006) needed to sustain abyssal mixing in the deep ocean. Previous studies have highlighted the importance of the wind for internal wave generation (D'Asaro 1985; Simmons and Alford 2012), a process that provides a mechanism for mixing through shear instabilities and wave breaking, often far away from the waves' generation region (Alford 2003b). The accurate estimation of this vertically propagating energy fraction is crucial for correctly representing abyssal mixing in general circulation and climate models.

The near-inertial band has been identified as important for transferring energy from inertial oscillations of the surface mixed layer, through the shear zone at the base of the mixed layer, and into vertical propagating near-inertial waves in the stratified ocean interior (e.g., Plueddemann and Farrar 2006). Multiple approaches have been taken to estimate how much energy the wind transfers to inertial oscillations of the surface mixed layer. D'Asaro (1985), in the first study of its kind, forced a slab model (Pollard and Millard 1970) with wind stress from moored meteorological buoys located in the North Pacific and North Atlantic to calculate the energy transfer from the wind to mixed layer currents rotating at the local inertial frequency. He showed that the bulk of the energy input was provided by midlatitude winter storms on scales of 100 km and was as such highly temporally intermittent. Building on this study, Alford (2001) produced maps of near-inertial wind power input between ±50° latitude, using 6-hourly NCEP–NCAR gridded reanalysis wind stress to force a slab model similar to D'Asaro (1985). He found significant regional and seasonal variability, with the wind supplying an average of about 0.29 TW to inertial oscillations of the

Denotes content that is immediately available upon publication as open access.

Corresponding author: Thilo Klenz, tklenz2@alaska.edu

DOI: 10.1175/JPO-D-21-0283.1

mixed layer, most of it being supplied in the western part of the basins during winter. Alford (2003a) later modified the slab model approach slightly and extended the Alford (2001) calculations poleward, estimating the global near-inertial wind power input to be around 0.47 TW. The ability of the slab model to accurately simulate mixed layer inertial currents as a response to strong wind forcing depends upon the suitability of the choices of prescribed mixed layer depth and a linear damping parameter (Alford 2020; Plueddemann and Farrar 2006). Plueddemann and Farrar (2006) showed that the slab model systematically overestimates near-inertial wind power input compared with observations, and hence questioned its utility for wind power calculations.

More recently, Alford (2020) updated the Alford (2003a) estimate again to 0.27 TW using hourly reanalysis winds and the Price et al. (1986) mixed layer model (henceforth referred to as the PWP model). Using the PWP model resulted in better agreement with observations compared to the slab model, due to an additional damping term acting on short time scales. Recently Alford (2020), using hourly, 0.6° resolution reanalysis winds, showed that the Pollard and Millard (1970) slab model overestimated near-inertial wind power input by 23% globally compared to PWP.

From the above estimates, the contribution of near-inertial wind power input is likely of the same order of magnitude as the estimated 1 TW provided by the tides (Jayne and St. Laurent 2001) and its importance in the global energy budget is clear. However, the large range of estimates from a variety of methods is evidence of significant uncertainty.

A desirable option is to use mixed layer velocities obtained from satellite-tracked Lagrangian surface drifters [see Niiler (2001) and Maximenko et al. (2013) for a review]. A large global array of approximately 1250 surface drifters is maintained as part of NOAA's Global Drifter Program (GDP; Centurioni et al. 2017). These drifters are drogued to follow the currents at 15-m depth and hence represent a good approximation of ocean mixed layer velocities. This fact together with their extensive coverage (Lumpkin et al. 2016), recently improved hourly reporting (Centurioni 2018), and the recent development of an enhanced resolution hourly interpolated product (Elipot et al. 2016), makes the GDP drifters convenient platforms for estimating near-inertial wind power input from observed mixed layer velocities directly, obviating the need for simulated velocities from a mixed layer model. Surface drifters have previously been utilized in combination with gridded wind products to estimate wind power input on regional and global scales. Elipot and Gille (2009b) used a subset of the standard, 6-hourly kriged GDP dataset (Hansen and Poulain 1996; Lumpkin and Pazos 2007) in combination with 6-hourly ERA-40 reanalysis wind stress to estimate wind power input in the Southern Ocean. On a global scale, Liu et al. (2019) used the hourly GDP dataset of Elipot et al. (2016) and a 6-hourly assimilated wind product. They estimated the global near-inertial wind power input to be between 0.3 and 0.6 TW, in general agreement with studies mentioned above.

The accuracy of gridded wind products in combination with surface drifters for near-inertial wind power calculations is, however, rarely assessed directly, particularly due to a lack of sufficient in situ wind measurements in combination with mixed layer current measurements. Schmidt et al. (2017) compared several gridded satellite scatterometer and reanalysis wind products to in situ winds measured from an autonomous measurement platform in the Southern Ocean. Their results emphasized the need for high resolution in situ wind measurements to validate gridded wind products. Liu et al. (2019) compared near-inertial wind power estimates calculated from surface drifters to that using in situ wind measurements from moored buoys located primarily in the North Atlantic and Pacific Oceans and found power estimates from 6-hourly reanalysis winds interpolated onto drifter positions were consistently smaller than those from moored buoy estimates by up to a factor of 2. They attributed this discrepancy to reduced near-inertial variance in the wind product. Similarly, Elipot and Gille (2009b) concluded that their near-inertial wind power calculations in the Southern Ocean are likely to be underestimates due to reduced near-inertial variance in both the 6-hourly drifter product and 6-hourly reanalysis winds (see also Gille 2005).

Since the transition to the Iridium satellite system in 2016, the modern GDP drifters have been configured to report their observations, including their GPS location, at regular hourly intervals (Centurioni 2018). The combination of hourly drifter data with a new generation of hourly reanalysis wind products promises significant improvements of the near-inertial wind power input estimate, particularly at latitudes above 50°, where the 6-hourly resolution of some gridded wind products is insufficient to resolve near-inertial wind variability due to the Coriolis frequency approaching the Nyquist frequency of the wind product (Alford 2001; Gille 2005). The hourly version of the GDP dataset has been shown to have between 25% and 50% more velocity variance than the previous, 6-hourly kriged version (Elipot et al. 2016). Flexas et al. (2019) showed that forcing their model with hourly instead of 6-hourly reanalysis winds resulted in an inertial peak in the surface current spectrum that was 2–3 times higher. While the hourly model reanalysis winds are definitely expected to result in improved near-inertial wind power input estimates, to our knowledge, an intercomparison between hourly model reanalysis winds and hourly in situ winds within the context of the near-inertial wind power problem has yet to be made. It is unclear whether the use of hourly reanalysis winds will solve problems associated with underestimated near-inertial variance, so validation against in situ measurements remains vital. This is the point of the present study.

In this study we utilize the Minimet drifter, a satellite-tracked, freely drifting measurement platform. Building on the Surface Velocity Program (SVP; Niiler et al. 1995; Niiler 2001; Centurioni 2018) drifter design, Minimet drifters (Centurioni 2018) were configured to measure in situ wind speed and direction at variable sampling rates in combination with position data. This presents us with a unique opportunity to estimate near-inertial wind power input from concurrent in situ wind and current measurements in the Lagrangian frame and compare it to that calculated using hourly ERA5 reanalysis winds interpolated along the Minimet drifter trajectories. To our knowledge, this is the first estimate of near-inertial wind power input using Lagrangian drifting buoys to provide both in situ current

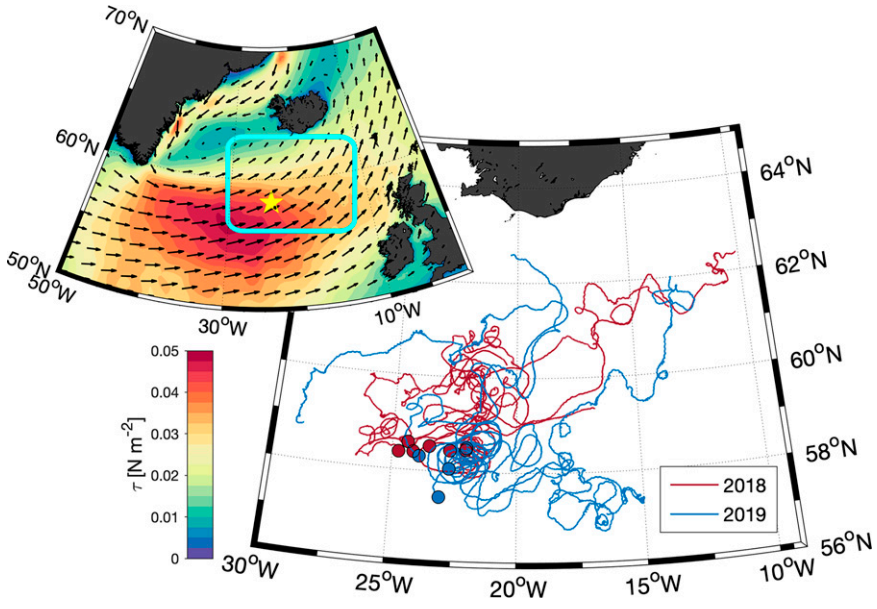

FIG. 1. Trajectories of Minimet drifters deployed during spring field campaigns in 2018 (red) and 2019 (blue). The inset shows the location of the study region and the time mean vector winds (arrows) and wind stress (colors) from ERA5 over the study period. Initial positions are shown by the colored dots and by the yellow star in the inset.

and wind measurements. The data and methods used for analysis are described in section 2, followed by our results and a discussion thereof in sections 3 and 4, respectively.

2. Data and methods

a. *Minimet surface drifters*

A total of 10 Minimet surface drifters were deployed from the R/V *Armstrong* during the Near-Inertial Shear and Kinetic Energy in the North Atlantic experiment (NISKINe). Five Minimets were deployed during each of the two cruises in May 2018 and June 2019 (Fig. 1). The Minimet (Centurioni 2018) is based on the SVP (https://gdp.ucsd.edu/ldl/svp/) drifter configuration, consisting of a surface float drogued with a holey sock at 15-m depth and equipped with a temperature sensor to measure sea surface temperature. Minimet drifter positions are tracked with a GPS transponder with 2–10-m accuracy, and data are transmitted using a two-way Iridium satellite modem. In addition to the standard SVP configuration, Minimets are equipped with a barometer and a 2D Gill Sonic anemometer, measuring wind speed up to 60 m s^{-1} and wind direction with 2% and ±2.5° accuracy, respectively, at a nominal height of 0.5 m above the sea surface. A 9-DOF (degrees of freedom) motion package is used to compute the attitude of the buoy with respect to the east-north-up (ENU) frame of reference. The 9-DOF chip's sensors are sampled simultaneously at high frequency and fed into a sensor fusion algorithm that outputs the 3D attitude of the buoy. The anemometer is sampled at the highest frequency allowed by the device and the horizontal wind is converted to the ENU frame of reference using the buoy orientation obtained from the motion package. The Minimet was designed to be deployed in front of tropical cyclones and is optimized to measure wind speed and direction in the most challenging conditions (Goni et al. 2017). Similar drifter configurations with an identical surface buoy design were successfully deployed in front of tropical cyclones and measured wind speeds in excess of 40 m s^{-1} (Hormann et al. 2014). An internal algorithm is used to filter out unrealistic or unrepresentative winds over a 7-min ensemble to ensure meaningful wind estimates. The wind velocity samples are discarded when the tilt of the sensor, obtained from the motion package, exceeds the manufacturer specifications, or when the anemometer is submerged. The wind samples are then preconditioned using a filter that removes anomalous wind velocity values due, for example, to wave crest shielding effects and disturbances from seawater spray, and wind speed is represented by the median value over the ensemble. This preprocessing aims to reduce bias due to the Minimet sampling in adverse conditions. Such a bias would be expected to lead to Minimet wind speed being lower at high wind speeds relative to reanalysis winds (cf. Large et al. 1995; Renfrew et al. 2020; Schmidt et al. 2017).

To assess how well the Minimets measure winds, Minimet wind speed measurements were compared against winds measured by the meteorology package on board the R/V *Armstrong* when the Minimets were within 25 km of the vessel during the respective cruise periods. True winds were calculated from raw R/V *Armstrong* ship winds following Smith et al. (1999) and the median was calculated over the same 7-min interval as the Minimets. Ship winds were adjusted from the ship-mast sensor height of 17.9 m to the standard 10-m height using an assumed law of the wall profile (Large and Pond 1981). The Minimet winds were similarly adjusted to 10 m by comparing the 10-m ship winds to the Minimet wind measurements

utilizing an iterative process that sought to minimize the root-mean-square deviation (RMSD) between the two measurements by varying the effective height of the Minimet wind sensor. The resulting Minimet effective sensor height of 0.30 m was subsequently used for adjusting the Minimet winds to 10-m height assuming a law of the wall (Large and Pond 1981).

Drifter velocities were obtained by central differencing the drifter positions in time. Outliers in the inferred velocity records were identified, and removed, in postprocessing by first applying a velocity standard deviation (σ) criteria to the Minimet velocity time series. Velocities exceeding 4σ were eliminated from the data. A second analysis step involved applying a 24-h running-mean filter to the drifter position time series and eliminating positions that deviated from the running mean by more than 0.05° in latitude or in longitude. The thresholds for these criteria were chosen subjectively. This procedure resulted in outliers being removed without damping high-frequency signals in the time series through excessive filtration. Minimet wind measurements for these outliers were discarded. After these processing steps, a total of 37 500 drifter hours of drifter velocities and in situ sea level winds from Minimet drifters deployed during the NISKINe cruise periods were available for analysis.

b. *Reanalysis winds*

We made use of the European Centre for Medium-Range Weather Forecasts (ECMWF) ERA5 reanalysis (ECMWF 2019). Hourly ERA5 10-m winds at 0.25° horizontal resolution were downloaded for the respective periods on 24 February 2020. As per the ERA5 documentation, timestamps can be viewed as instantaneous, with winds available at the top of the hour, matching the temporal resolution of the Minimets. To calculate near-inertial wind power input and for comparison to in situ measurements, ERA5 10-m winds were linearly interpolated onto drifter GPS positions at every time step. It is important to note that while sea level pressure measurements from the Minimets were assimilated into the reanalysis, the wind measurements were not, therefore ensuring that the ERA5 winds are independent from our in situ measurements.

c. *Near-inertial wind power calculation*

Near-inertial wind power input was estimated by first calculating wind stress $\boldsymbol{\tau}$ along the drifter trajectories. Since the Minimets essentially measure wind speed relative to the ocean velocity at 15-m depth, we can calculate the wind stress as

$$\boldsymbol{\tau}_{\mathrm{mm}} = c_d \rho_{\mathrm{air}} \|\tilde{\mathbf{u}}_{\mathrm{mm}}\| \tilde{\mathbf{u}}_{\mathrm{mm}}, \tag{1}$$

with $\|\tilde{\mathbf{u}}_{\mathrm{mm}}\|^2 \equiv \tilde{\mathbf{u}}_{\mathrm{mm}} \cdot \tilde{\mathbf{u}}_{\mathrm{mm}}$. Here, $\tilde{\mathbf{u}}_{\mathrm{mm}}$ is the horizontal wind vector from Minimet wind measurements adjusted to 10-m height, ρ_{air} is a reference air density assumed to be a constant at 1.25 kg m^{-3}, and c_d is a drag coefficient obtained following Large and Pond (1981). To compare ERA5 winds to in situ winds from the Minimets, we have to subtract the drifter velocities from the reanalysis winds and calculate ERA5 wind stress as follows:

$$\boldsymbol{\tau}_{\mathrm{era}} = c_d \rho_{\mathrm{air}} \|\tilde{\mathbf{u}}_{\mathrm{era}} - \mathbf{u}\| (\tilde{\mathbf{u}}_{\mathrm{era}} - \mathbf{u}). \tag{2}$$

Here $\mathbf{u}$ is a vector of the drifter velocity at 15-m depth, which we assume to be an adequate approximation of the surface currents, and $\tilde{\mathbf{u}}_{\mathrm{era}}$ is the 10-m wind vector from ERA5. Flexas et al. (2019) highlighted the importance of including the effect of ocean currents in calculating the wind stress, and Alford (2020) and Rath et al. (2013) reported a reduction of wind power input into the near-inertial band of 13% and 20%, respectively, when accounting for this effect. Energy input by the wind can be calculated as the time integral of Π over some time interval.

Trajectories were divided into 20-day segments with 50% overlap. The segment length was chosen to account for the change of Coriolis parameter along a given trajectory while retaining adequate frequency resolution. Near-inertial wind power input Π was then calculated for each 20-day segment by multiplying wind stress $\boldsymbol{\tau}$ calculated using either Eq. (1) or Eq. (2) along the drifter trajectory by the near-inertial drifter velocity $\mathbf{u}_I$:

$$\Pi = \boldsymbol{\tau} \cdot \mathbf{u}_I. \tag{3}$$

The velocity $\mathbf{u}_I$ was calculated using a bandpass filter. The specific choice of filter will be described in detail later on.

3. Results

As mentioned previously, a total of 10 Minimet drifters were deployed from the R/V *Armstrong* during NISKINe Pilot and Process cruises in spring of 2018 and 2019 (Fig. 1). All Minimets recorded their positions, as well as in situ sea surface wind speed and direction, for several months, 156 days on average. The Minimets were deployed in an active mesoscale eddy field and hence experienced rapid dispersal over their lifetimes, drifting in a mainly northeasterly direction from their initial deployment locations. Individual Minimet drifters occasionally became trapped in eddies, particularly around 58°N and 22°W, as indicated by their looping trajectories. The study region in which the Minimets were deployed was characterized by strong wind stress (Fig. 1, inset), with winds mainly from a southwesterly to westerly direction. As such, Minimet drifters would routinely undergo inertial oscillations forced by passing storms, as can be seen upon zooming into Fig. 1 (not shown).

To evaluate the utility of Minimet wind measurements, in situ wind speed measured by Minimet drifters and by the meteorological package located on the bow of the R/V *Armstrong* are compared during the respective cruise periods. We are comparing measurements during times when both platforms were within 25 km of each other, resulting in a total of 1137 individual wind speed data pairs recorded at 15-min intervals. For quality-control purposes, ship winds were omitted following Smith et al. (1999) during times when the ship was rapidly changing course, accelerating or decelerating, or when the true wind direction was within ±15° of the stern of the ship. Changing this true wind direction criterion to ±30° reduced the number of data points but did not significantly alter the results. The two measurements agreed well with each other (Fig. 2a) and the majority of measurements lay on or close to the 1:1 line (Fig. 2b), with wind speeds up to 17 m s^{-1} captured by both.

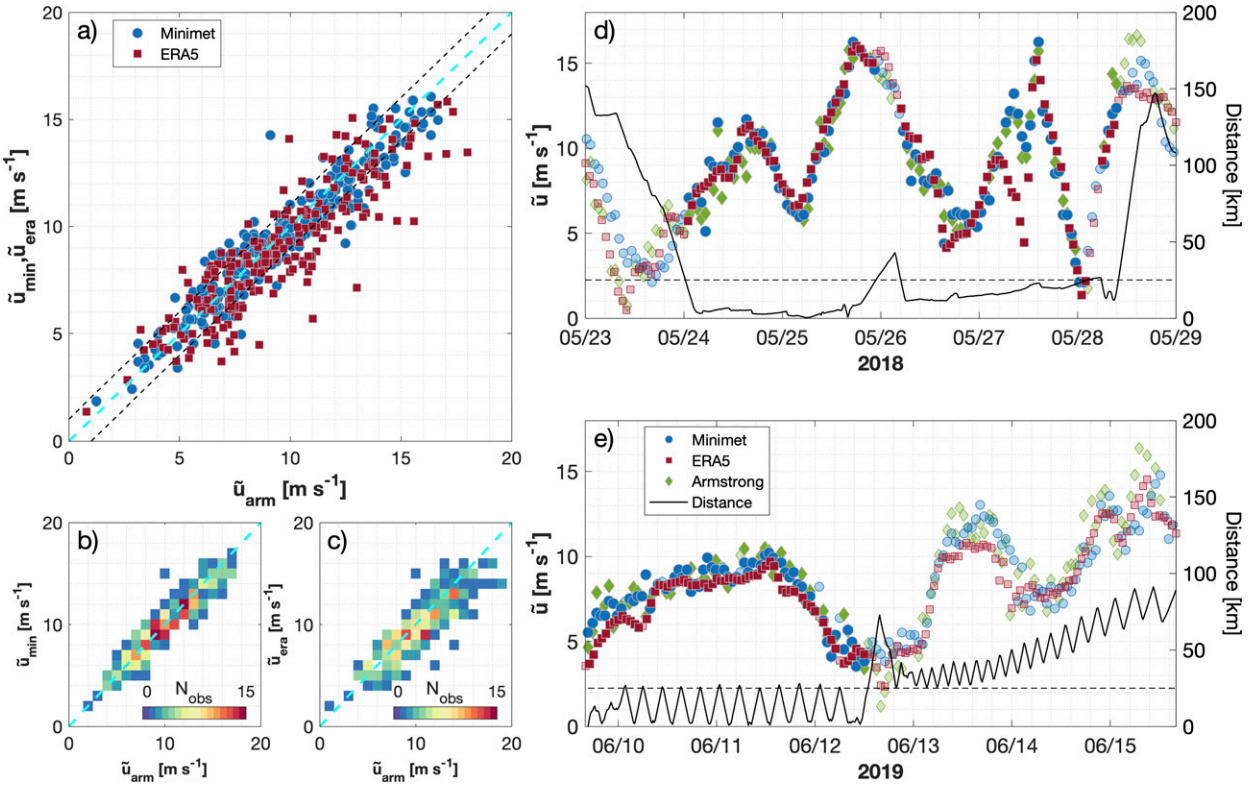

FIG. 2. (a) Coincident Minimet (blue) and ERA5 (red) wind speed vs R/V *Armstrong* wind speed. Minimet winds within 25 km of R/V *Armstrong* were considered. (b) Number of observations for Minimet vs *Armstrong* winds in 1 m s^{-1} bins. (c) As in (b), but for ERA5 vs *Armstrong* winds. (d) Time series of hourly wind speed from a single Minimet (blue circles), R/V *Armstrong* (green diamonds) and ERA5 reanalysis interpolated onto the vessel's position (red squares) during the 2018 Pilot cruise. The distance between the respective Minimet drifter and R/V *Armstrong* is shown in black, and the black dotted line depicts 25-km distance. Opacity indicates when the Minimet is within 25 km of R/V *Armstrong*. (e) As in (d), but during the 2019 Process cruise.

ERA5 winds interpolated onto the position of R/V *Armstrong* revealed that ERA5 wind speed generally tended to be lower than that from R/V *Armstrong* (Figs. 2a,c) for the same times considered in the Minimet and R/V *Armstrong* comparison.

Time series of adjusted 10-m wind speed indicate that wind speeds from all three sources generally agreed well during times when Minimets and the research vessel were within 25 km of each other (Figs. 2d,e), while, unsurprisingly, agreement between Minimets and R/V *Armstrong* winds generally worsened with increasing distance. Temporal variability as well as the magnitude of wind events was generally well captured by all. However, during individual high wind events, ERA5 reanalysis wind speed was significantly lower compared to that measured from R/V *Armstrong* and the Minimets, as was evident during wind events on 27 May 2018, 28 May 2018 (Fig. 2d), and 13 June 2019 (Fig. 2e). During these wind events, ERA5 wind speed differed from R/V *Armstrong* by up to 5 m s^{-1} while wind speed differences between Minimets and R/V *Armstrong* were smaller.

To quantify the wind speed differences between Minimets, ERA5, and R/V *Armstrong*, we compute the mean square deviation (MSD) between wind speeds sorted into wind speed bins of 1 m s^{-1}. The MSD is further separated into two components, the square of the bias (systematic differences) and variance (spread around the mean). The term bias is used in a strict statistical sense, with no assumption about which measurement platform represents the true wind speed. These intercomparisons during the cruise periods aid in evaluating the observed differences between ERA5 and Minimet wind speed during the entire observation period.

Wind speed differences between Minimets and R/V *Armstrong* when both were within 25 km of each other were generally small, 1 m s^{-1} at wind speeds of 17 m s^{-1} (Fig. 3a). Differences between ERA5 and R/V *Armstrong* during those times were larger, around 2–4 m s^{-1} in the same wind speed range (cf. Fig. 2). Wind speed differences generally increased with wind speed. Over the whole observation period, ERA5 and Minimets wind stress differences increased linearly to about 1 m s^{-1} for wind speeds up to 20 m s^{-1}, indicating that ERA5 wind speed was generally lower than that from Minimets. For wind speed in excess of 20 m s^{-1}, ERA5 wind speed differed from Minimet wind speed by up to 3 m s^{-1}. Note that wind speeds in excess of 20 m s^{-1} were only observed for 0.5% of the Minimet data (not shown) and were hence very rare. However, comparable wind speed differences between ERA5 and R/V *Armstrong* were observed during the cruise periods for wind speeds of 10–20 m s^{-1}.

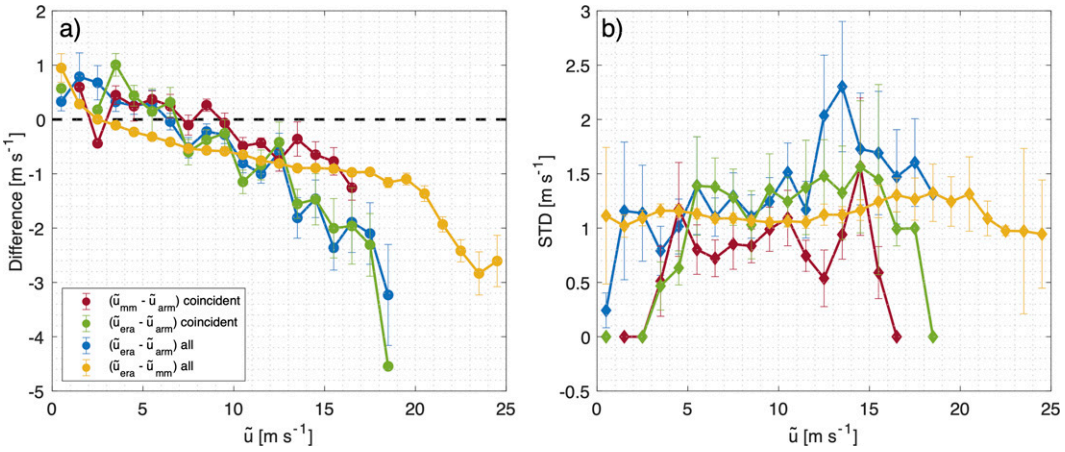

FIG. 3. (a) Wind speed difference between Minimet and R/V *Armstrong* wind speed measurements during the cruise periods when Minimets were within 25 km of R/V *Armstrong* (red), between ERA5 and R/V *Armstrong* wind speed values for times when Minimets were within 25 km from R/V *Armstrong* (green), between all ERA5 and R/V *Armstrong* wind speed values during the whole cruise periods (blue), and between all ERA5 and Minimet wind speed values during the whole observation period (yellow). (b) Wind speed standard deviation between wind speed values according to the legend in (a). Error bars in all panels depict the standard error, and wind speed differences and standard deviations are plotted against the respective reference wind speed measurement, either from R/V *Armstrong* (red, green, blue) or the Minimets (yellow).

The standard deviation (calculated as the square root of the variance) between Minimet and R/V *Armstrong* wind speed was 0.97 m s^{-1} when both platforms were within 25 km of each other (Fig. 3b). In comparison, for ERA5 wind speed values interpolated onto Minimet positions and coincident with Minimet wind measurements within 25 km of R/V *Armstrong* the standard deviation between Minimet wind speed and ERA5 wind speed was 1.22 m s^{-1} (cf. Fig. 2). Over the entire observation period, the standard deviation between Minimet and ERA5 wind speed was 1.26 m s^{-1}. Both the observed differences and standard deviations between Minimets and R/V *Armstrong* wind speed suggest that the two measurements agreed well, while agreement between ERA5 and R/V *Armstrong* was poorer, leading us to conclude that the Minimet winds are reliable.

We want to further investigate the differences between ERA5 and Minimets at high wind speeds by highlighting an energetic wind event in August 2018 that was sampled by four of five Minimets (Fig. 4). Peak wind speed for this wind event as measured by the Minimets on 17 August 2018 was around 20 m s^{-1}. The Minimets here are numbered 1–5 for the sake of simplicity. During this wind event, the center of the cyclone moved eastward just north of the Minimets, with maximum wind stress passing directly over four of the five Minimets (Fig. 4a). Minimets 1–3 encountered maximum wind stress at 1700 UTC 17 August 2018, while Minimet 5 was furthest to the west and sampled the same wind event slightly earlier. The largest difference between wind stress estimated from Minimet winds and ERA5 winds was found for Minimets 1 and 3. However, these Minimets, being closest to the center of the cyclone, were sampling in regions characterized by large local gradients in the reanalysis wind field. Additionally, Minimets 2 and 5, which were sampling furthest from the center of the cyclone and in a region of less pronounced local gradients, recorded wind stress equal to or larger than the reanalysis model. This suggests the possibility that a mismatch of the spatial location of maximum winds between the observations and the reanalysis model could account for the differences between the reanalysis winds and those observed by the Minimets.

To further examine this hypothesis, we can look at wind speed differences between ERA5 and Minimets in the vicinity of wind speed gradients in the ERA5 reanalysis fields. We find that differences between the two are larger in the vicinity of larger local horizontal gradients in the ERA5 wind field (Fig. 5). Further, spatial gradients in the ERA5 fields map onto the time domain, and, because these energetic storms are translating rapidly, a simple gradient analysis addresses both spatial and temporal discrepancies. This leads us to conclude that the observed differences between individual events in the Minimet and ERA5 data could at least in part be explained by a difference in spatial structure of individual wind events between observations and the reanalysis model, or a potential lack of small-scale structure in the reanalysis model fields.

Having established how Minimet and ERA5 winds differ, we want to investigate the impact of these differences on the near-inertial wind power input calculations. First of all, near-inertial wind power input into the ocean can be represented as a time series by calculating the dot product in Eq. (3) or in frequency space, through the real part of the complex cross spectrum between the wind stress and the surface velocities (Elipot and Gille 2009a; Flexas et al. 2019), as will be further investigated later. Hence, it makes sense to first look at the frequency-domain representation of the drifter velocities and wind stress from both ERA5 and Minimets.

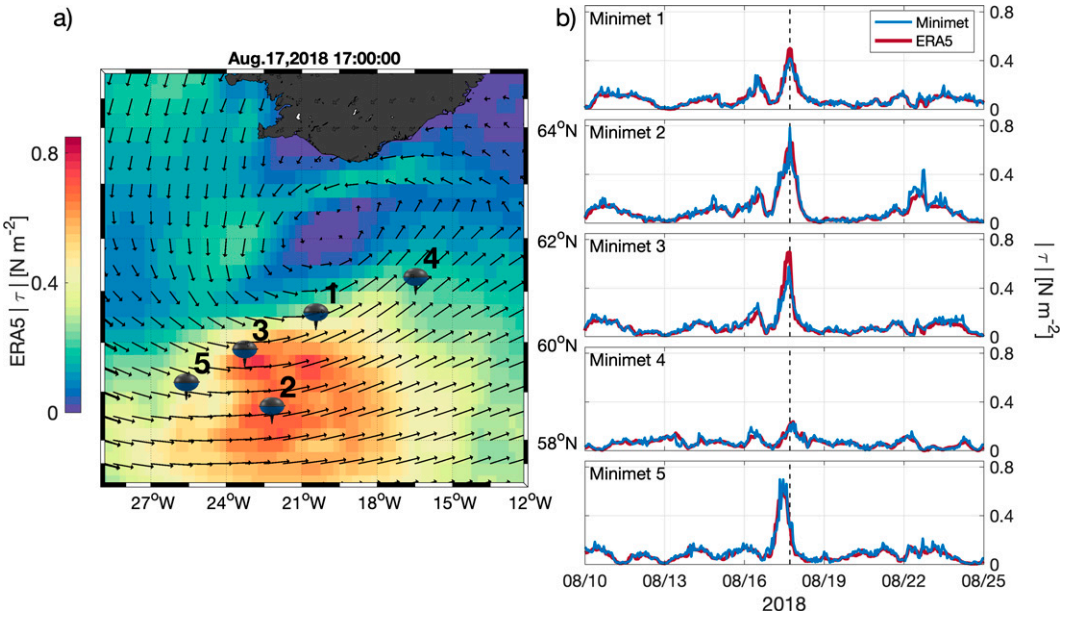

FIG. 4. (a) Wind stress (colors) and wind vectors (arrows) from ERA5 at 1700 UTC 17 Aug 2018. The locations of five Minimets are shown. (b) Time series of wind stress from Minimet winds (blue) and ERA5 winds (red) for each of the five Minimets shown in (a). The vertical black dashed line corresponds to the time of the peak of the event shown in (a).

We estimated rotary spectra for 20-day segments of Minimet and ERA5 winds, as well as Minimet drifter velocities, by first multiplying each 20-day time series by a Slepian taper (Slepian 1978), calculating the Fourier transform, and taking the squared modulus of the result. The time-bandwidth product p was chosen to be $p = 2$. A total of 138 twenty-day, half-overlapping segments were then averaged to produce the spectral estimates and frequencies were normalized by the mean inertial frequency f_0 along the respective 20-day trajectory segments (Fig. 6). Since both the Minimet measurements and ERA5 reanalysis had hourly resolution, the Nyquist frequency was $\omega_{Ny} = 12$ cpd, far from the average inertial frequency over the entire record of 1.7 cpd.

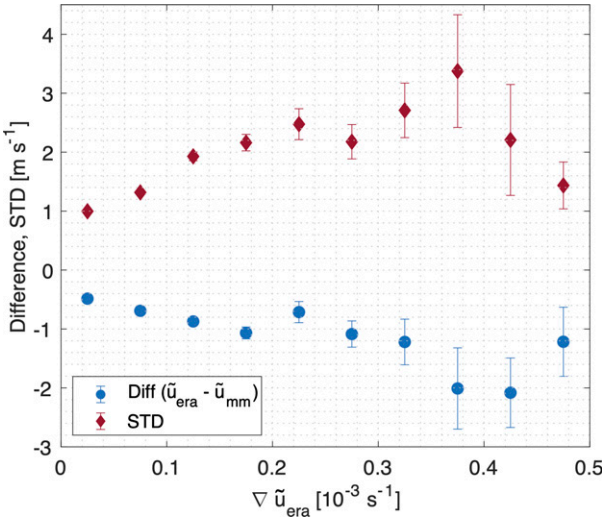

FIG. 5. Wind speed difference (blue circles) and standard deviation (red diamonds) between Minimet and ERA5 vs the local ERA5 wind speed gradient magnitude in the vicinity of the Minimets. Error bars depict the standard error.

Both wind stress spectra were red, but Minimet wind stress showed a significantly shallower spectral slope at high frequencies compared to ERA5 (Fig. 6a). Around the inertial frequency the two spectra start to diverge, with spectral energy at the local inertial frequency higher in the Minimet data compared to ERA5 winds by a factor of 1.8 (Fig. 6a, inset). Spectral energy at superinertial frequencies up to the Nyquist frequency was significantly larger in the Minimet dataset compared to ERA5. There is no reason to believe that this difference at superinertial frequencies is due to noise in the Minimet wind data. Rather, it is indicative of the Minimets capturing high-frequency variability related to wind events happening on time scales smaller than the inertial period that are seemingly not captured in the ERA5 model.

Minimet drifter velocities are used to estimate near-inertial wind power input in combination with both Minimet winds and ERA5 reanalysis winds. Their rotary spectra (Fig. 6b) showed a distinct peak around the average inertial frequency f_0 on the clockwise side of the rotary spectrum, as expected for these Northern Hemisphere drifters, while a peak at the semidiurnal tidal frequency dominated the counterclockwise side. A superinertial shoulder on the clockwise side of the velocity rotary spectrum coincides with the semidiurnal tidal frequency. This shoulder is an order of magnitude larger than the semidiurnal peak on the counterclockwise side and is

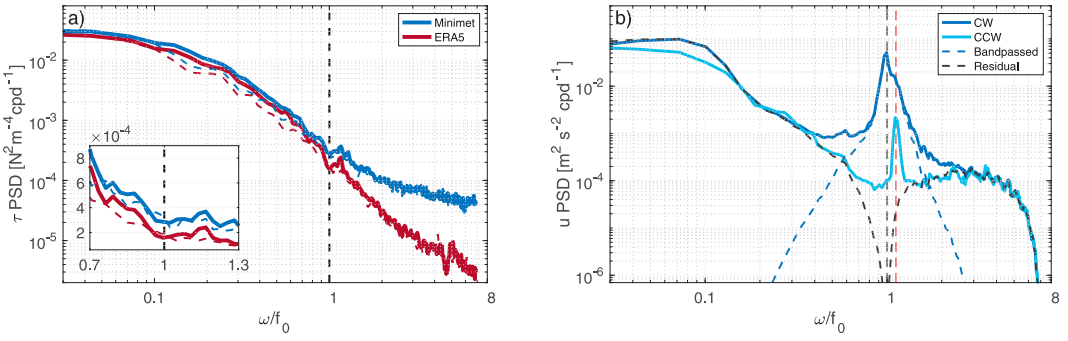

FIG. 6. (a) Wind stress rotary spectra for Minimet in situ winds (blue) and ERA5 reanalysis winds (red). Solid and dashed lines represent the clockwise and counterclockwise sides of the rotary spectrum, respectively. The inset highlights the near-inertial regime between $0.7 \leq \omega/f_0 \leq 1.3$ on linear axes. (b) Clockwise (dark blue) and counterclockwise (light blue) rotary spectral components for drifter velocities. The dashed blue line shows the effect of the bandpass applied to the clockwise side of the spectrum and the dashed black line shows the clockwise rotary spectral component of the residual velocities obtained by subtracting the bandpassed velocities. The vertical dashed red line marks the location of the M_2 tidal frequency.

indicative of an anticyclonic polarization of the semidiurnal tide. A small peak at $\omega = 0.6f_0$ coincides with the diurnal tide.

To calculate near-inertial wind power input using Eq. (3), drifter velocities were bandpassed using a generalized Morse wavelet filter (Lilly 2017), applied only to the anticyclonic side of the drifter velocity rotary spectrum. The parameters of the filter were chosen subjectively as $\gamma = 0.4$ and $\beta = 12$ in order to effectively eliminate the observed inertial peak (Fig. 6b, gray dotted line). The advantage of using such a one-sided bandpass is that energy on the cyclonic side, rotating opposite the inertial oscillations, is completely eliminated and hence does not contaminate the estimates. The resulting bandpassed drifter velocities captured the spectral energy in the near-inertial band around the local inertial frequency f_0 on the clockwise side of the rotary spectrum (Fig. 6b, blue dotted line), while excluding such energy from the residual velocities, that is, the original signal minus the bandpass. It should be noted that our filter does not eliminate the semidiurnal tidal signal on the clockwise side of the rotary spectrum.

We now want to highlight two wind events that are representative of when differences between ERA5 and Minimet-derived near-inertial wind power estimates arise. Example time series of bandpassed drifter velocities, Minimet and ERA5 wind stress magnitude, and the associated estimated near-inertial wind power and energy input for two wind events captured by Minimets in August 2018 and October 2019 are shown (Fig. 7). In these example time series, Minimet drifters underwent inertial oscillations forced by wind events around 18 August 2018 and 7 October 2019 (Figs. 7a,b). There is indication of the semidiurnal tide being present in the bandpassed drifter velocities and of possible leakage from the diurnal tide (cf. Fig. 6b), particularly when the inertial signal is weak and the tides might dominate. While both ERA5 and Minimets seem to capture the general temporal variability well, Minimet wind stress magnitude was lower compared to ERA5 wind stress in 2018 and higher in 2019 (Figs. 7c,d), and high-frequency variability was more pronounced in the Minimet winds. The onset of inertial oscillations with peak amplitudes of 0.28 and 0.2 m s^{-1} (Figs. 7a,b) coincided with the wind events in August 2018 and October 2019, respectively. Near-inertial wind power Π during the event in 2018 showed a distinct peak corresponding to this short-lived wind event, while near-inertial wind power amplitude remained high for several days due to the prolonged high wind stress following the onset of the event in 2019 (Figs. 7e,f). Additionally, peak Minimet wind stress during the 2019 wind event was delayed by 8 h compared to ERA5, as can be seen by zooming into Fig. 7d (not shown). Peak Minimet wind stress coincided with maximum inertial current amplitude and consequently lead to larger near-inertial wind power input compared to ERA5 (Fig. 7f). Time-averaged estimated near-inertial wind power input $\langle\Pi\rangle$ from Minimet and ERA5 winds over the two periods considered were $\langle\Pi\rangle_{MM} = 0.4$ mW m^{-2} and $\langle\Pi\rangle_{ERA} = 0.9$ mW m^{-2} between 10 and 25 August 2018, and $\langle\Pi\rangle_{MM} = 1.2$ mW m^{-2} and $\langle\Pi\rangle_{ERA} = 0.4$ mW m^{-2} between 3 and 18 October 2019. Minimet-derived energy input into the mixed layer estimated along the Minimet trajectories over the same time period was about 2.3 times lower in August 2018, and about 3.7 times higher in October 2019 (Figs. 7g,h) compared to that calculated from ERA5 winds. The impact of the two wind events presented here was a net input of energy into the ocean by the winds as captured by both the Minimet and ERA5 winds, but their magnitudes differ substantially.

The two example time series above (Fig. 7) highlight one case in which ERA5 overestimates, and one case in which it underestimates, the time-averaged near-inertial wind power input relative to that computed using the Minimet winds. Over the whole dataset, the time-averaged near-inertial wind power input $\langle\Pi\rangle$ estimated from Minimet winds was 0.26 ± 0.06 mW m^{-2}, 42% higher than the 0.18 ± 0.05 mW m^{-2} estimated from ERA5 winds. For both Minimet and ERA5 winds the estimated effect of the wind acting on the ocean surface was, unsurprisingly, a net input of power into the ocean over the observation period considered here.

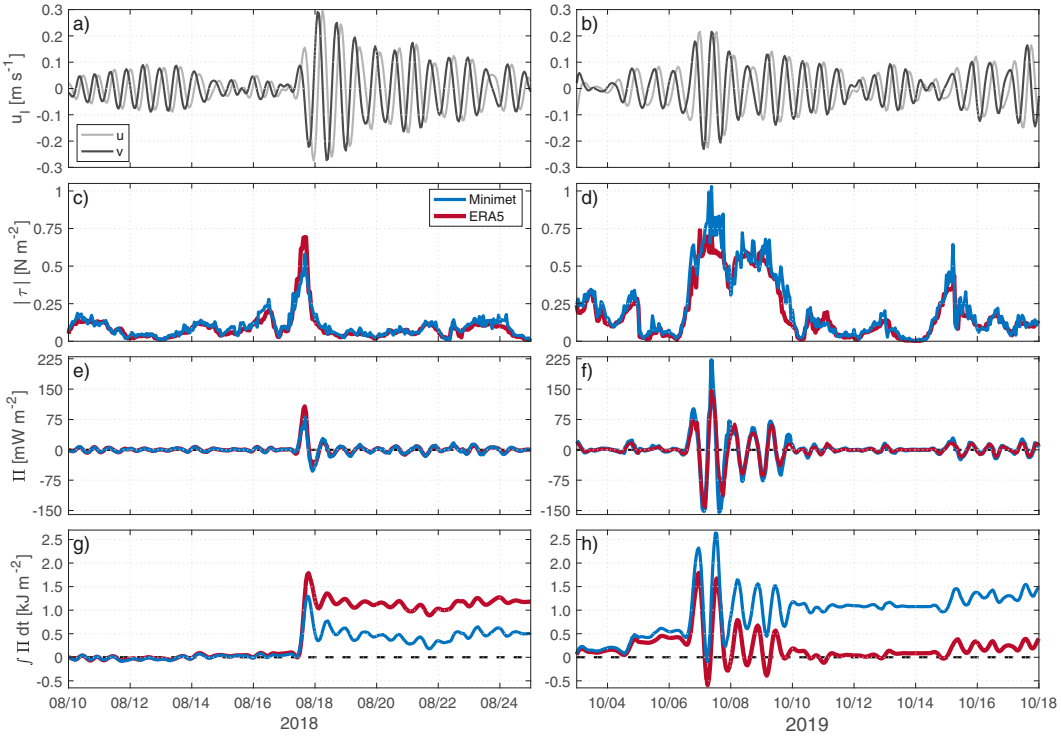

FIG. 7. Example time series for two wind events recorded in (left) August 2018 and (right) October 2019. Shown are (a),(b) bandpassed near-inertial currents from the Minimets, (c),(d) wind stress magnitude calculated from Minimet winds (blue) and ERA5 reanalysis winds (red), (e),(f) near-inertial wind power input, and (g),(h) energy input.

To investigate how the wind-speed-dependent differences in wind speed presented above affect the near-inertial wind power input estimates, we averaged instantaneous near-inertial wind power input differences between Minimets and ERA5 in 1 m s^{-1} wind speed bins. At wind speeds below 20 m s^{-1} these differences were small and largely negative, indicating that Minimet-derived estimates were generally larger than those from ERA5 winds (Fig. 8a). Significantly larger differences between the two estimates were apparent at wind speeds larger than 20 m s^{-1} (Fig. 8a). However, these were again associated with rare events. The bulk of the discrepancy in time-averaged near-inertial wind power input from Minimets

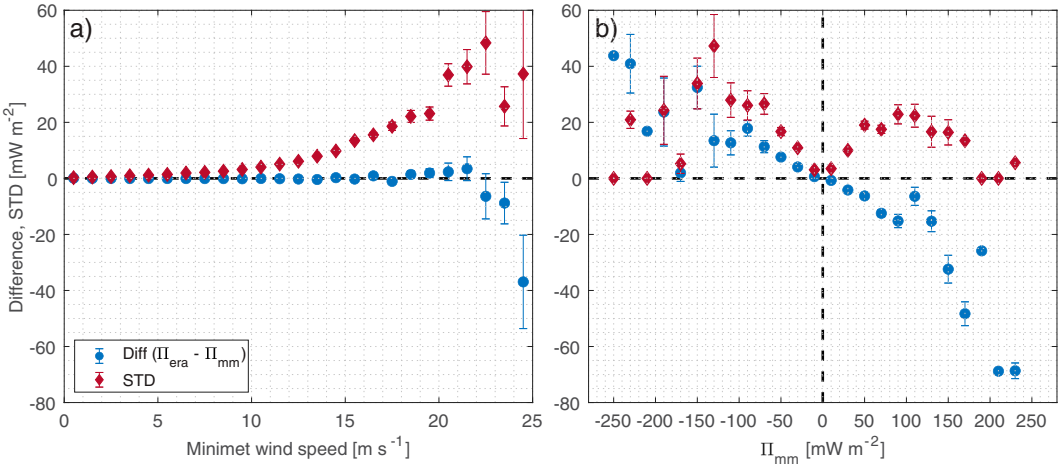

FIG. 8. (a) Instantaneous near-inertial wind power input difference and standard deviation between ERA5 and Minimet-derived near-inertial wind power input estimates vs Minimet wind speed in 1 m s^{-1} bins. (b) As in (a), but plotted against instantaneous Minimet-derived near-inertial wind power input estimates in 20 mW m^{-2} bins. Error bars in both panels denote the standard error.

and ERA5 stems from the differences at smaller wind speeds, with Minimet-derived time-averaged near-inertial wind power input for wind speeds below 20 m s^{-1} being larger than that estimated from ERA5 winds by 75%. At wind speeds larger than 20 m s^{-1}, time-averaged near-inertial wind power estimated from Minimets was larger by only 10%.

Standard deviation between instantaneous near-inertial wind power input estimates increased for wind speeds larger than 10 m s^{-1} suggesting that, while differences averaged in wind speed bins below 20 m s^{-1} were small and generally indicating near-inertial wind power input estimated from Minimets to be larger than that from ERA5, discrepancies grew more pronounced with increasing wind speed.

Near-inertial wind power input differences averaged in instantaneous Minimet-derived near-inertial wind power input bins showed that particularly at the high positive and negative ends of the distribution, Minimet-derived estimates showed considerably larger near-inertial wind power input magnitudes compared to those estimated from ERA5 winds (Fig. 8b). ERA5 underestimated both energy input and energy loss, with the former being more pronounced. Some physical intuition might help interpret this effect. Strong wind events happening on time scales shorter than an inertial period could lead to large near-inertial wind power input during the first half of an inertial period, when winds and currents are in phase. Differences in wind speed magnitude or the onset of these wind events between the Minimet observations and ERA5 data could explain the asymmetry in Fig. 8b.

To investigate the short-time-scale hypothesis further, we now look at time scales over which differences between ERA5 and Minimet winds contributed to the observed near-inertial wind power input discrepancies. We analyzed those events during which instantaneous near-inertial wind power input estimates in the Minimet record differed from the record mean by more than one standard deviation

$$|\Pi_{\mathrm{mm}} - \langle \Pi_{\mathrm{mm}} \rangle| > \sqrt{\frac{1}{N}\sum (\Pi_{\mathrm{mm}} - \langle \Pi_{\mathrm{mm}} \rangle)^2}, \qquad (4)$$

and also simultaneously during which the difference between instantaneous Minimet and ERA5 near-inertial wind power input estimates was greater than one root-mean-square deviation

$$|\Pi_{\mathrm{mm}} - \Pi_{\mathrm{era}}| > \sqrt{\frac{1}{N}\sum (\Pi_{\mathrm{mm}} - \Pi_{\mathrm{era}})^2}. \qquad (5)$$

In both criteria N represents the record length. Testing the entire record for (4) and (5) identified those energetic wind events that contributed to significant differences in time-averaged near-inertial wind power input estimates from Minimet and ERA5 winds. Their duration is defined as the number of consecutive hours during which both of the above criteria were met.

The bulk of events that contributed most to the observed discrepancies happened on time scales much shorter than the local inertial period (Fig. 9), with many individual events lasting less than half an inertial period, further highlighting the importance of accurately capturing energetic wind events occurring on time scales smaller than the local inertial period to accurately represent near-inertial wind power input, as noted previously by Plueddemann and Farrar (2006).

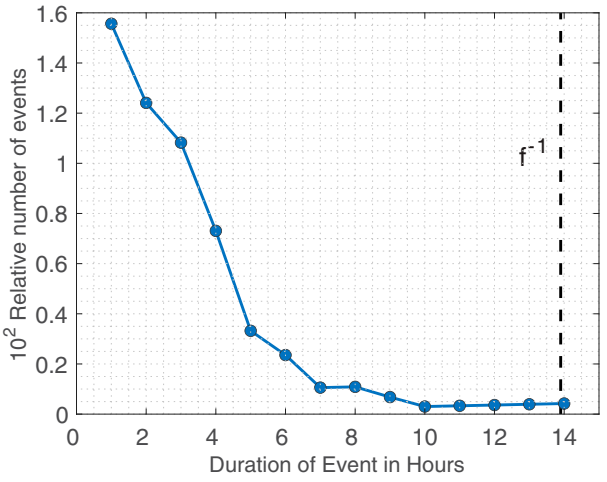

FIG. 9. Relative number of events lasting between 1 and 14 h contributing to the discrepancy between Minimet and ERA5 near-inertial wind power input, defined as Π_{mm} varying by more than one standard deviation from the record mean and estimates of instantaneous wind power input Π from Minimet and ERA5 winds differing by more than one root-mean-square deviation. The average Coriolis period over the record is shown by the black dashed line.

To investigate the frequency-domain representation of near-inertial wind power input into the mixed layer, we calculate complex-valued rotary cross spectra between wind stress and drifter velocities. Lilly and Elipot [2021, their Eq. (12)] have shown that under the assumptions of the Ekman problem, the rate of change of the vertically integrated mixed layer kinetic energy due to the wind forcing is given by

$$\Re\{\tau(t)u^*(t)\} \equiv \Pi(t). \qquad (6)$$

Here $\tau(t)$ and $u(t)$ are complex-valued time series of the form $z(t) = x(t) + iy(t)$, with $x(t)$ being the zonal and $y(t)$ the meridional components of the drifter velocity or wind stress vector, and $(\cdot)^*$ denotes the complex conjugate. Equation (6) is thus interpreted as the instantaneous wind power input. We can express the wind stress and drifter velocities as their spectral representations

$$\tau(t) = \frac{1}{2\pi}\int_{-\infty}^{\infty} e^{i\omega t} dT(\omega) + \overline{\tau},$$

$$u(t) = \frac{1}{2\pi}\int_{-\infty}^{\infty} e^{i\omega t} dU(\omega) + \overline{v},$$

[Lilly and Elipot 2021, their Eqs. (2) and (3)] and substitute them into the definition of the cross covariance:

$$R_{\tau u}(\nu) \equiv E[\tau(t)u^*(t - \nu)].$$

Together with the definition of the cross spectrum

$$S_{\tau u}(\omega)\delta(\omega - \upsilon)d\omega\, d\upsilon \equiv \frac{1}{2\pi}E[dT(\omega)dU^{*}(\upsilon)],$$

we readily obtain

$$R_{\tau u}(\nu) = \frac{1}{2\pi}\int_{-\infty}^{\infty} e^{i\omega\nu}S_{\tau u}(\omega)d\omega,$$

which states that the cross covariance and the cross spectrum are a Fourier transform pair (Emery and Thomson 2001). Combining this with Eq. (6) we see that the time-averaged wind power input is given by

$$\langle \Pi \rangle \equiv E[\Pi(t)] = E[\Re\{\tau(t)u^{*}(t)\}] = R_{\tau u}(0)$$
$$= \frac{1}{2\pi}\int_{-\infty}^{\infty} \Re\{S_{\tau u}(\omega)\}d\omega.$$

This implies that the total expected wind power input is the integral of the real part of the cross spectrum, the cospectrum, between the wind stress and the surface current, and contributions due to fluctuations in the vicinity of the local inertial frequency can be obtained by bandpassing either the wind stress or the surface currents.

We estimated complex-valued rotary cross spectra by first multiplying each 20-day segment of Minimet wind stress, ERA5 wind stress, and Minimet drifter velocities with a Slepian taper (Slepian 1978). The time–bandwidth product p was again chosen to be $p = 2$. Shown here is only the clockwise side of the cospectrum; the counterclockwise side showed little to no spectral energy in the near-inertial band, as is expected since inertial oscillations rotate clockwise in the Northern Hemisphere.

Cospectra averaged over all available segments from both Minimet and ERA5 winds showed a local maximum at or around the local Coriolis frequency, with maximum cospectral values at $\omega/f_0 = 1$ being larger by a factor of 2.4 for those estimated from Minimet winds compared to those from ERA5 winds (Fig. 10). Since wind stress spectra differed by only a factor of 1.8 at $\omega/f_0 = 1$ (Fig. 6a), the larger discrepancy in the cospectra is indicative of larger coherence between the Minimet drifter velocities and Minimet winds compared to ERA5 winds (not shown). Between $0.7f_0$ and $0.95f_0$ the ERA5 cospectrum was larger compared to the Minimet-derived estimate. At superinertial frequencies both cospectra were negative, particularly around $1.11f_0$, indicating the wind essentially removing energy from the ocean at these frequencies. Negative cospectra at $1.11f_0$ for both the Minimet and ERA5 winds coincide with the superinertial shoulder on the clockwise side of the velocity rotary spectrum and a spectral peak on the counterclockwise side (Fig. 6b, red dashed line), suggesting that the wind acting on the semidiurnal tide could act to remove energy from the ocean. For frequencies $\omega \gg f_0$, cospectral values were nearly equal to zero for both Minimet and ERA5 estimates.

4. Discussion

Novel in situ wind measurements from Lagrangian Minimet surface drifters were validated against coincident ship wind measurements, as suggested by Schmidt et al. (2017) as a method to verify in situ measurements from platforms such as the Minimet. While ship winds are not without issues (e.g., Landwehr et al. 2020; Smith et al. 1999), they provide an additional independent wind measurement in the vicinity of the Minimets and aid in evaluating the wind speed differences observed between ERA5 and Minimet winds outside of the cruise periods. Comparisons to R/V *Armstrong* winds during the cruise periods indicated that Minimet winds differed slightly from ship winds, with both positive and negative differences of up to 1 m s^{-1} occurring over the observed wind speed range up to 17 m s^{-1}. However, considering these measurements were separated by up to 25 km, we would not expect them to agree perfectly. Overall, validation against independently measured ship winds have shown that Minimets captured the general temporal variability and wind speed magnitude well.

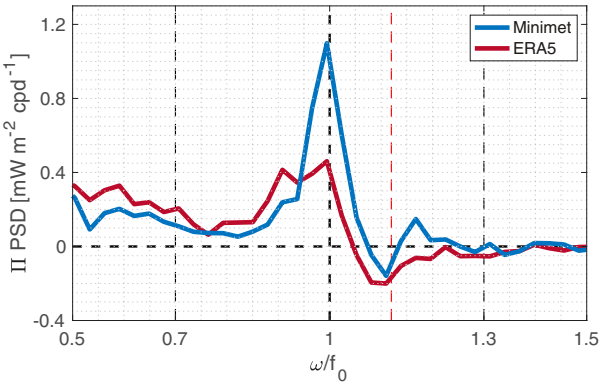

FIG. 10. Coincident clockwise rotary spectrum between Minimet drifter velocities and Minimet winds (blue) and between Minimet drifter velocities and ERA5 winds (red). The near-inertial frequency band between $0.7f_0$ and $1.3f_0$ is indicated by the vertical thin black dotted lines and the vertical dashed red line marks the location of the M_2 tidal frequency (cf. Fig. 6b).

Potential problems with platforms like the Minimet measuring winds close to the sea surface include a sheltering effect by wave crests and the periodical submersion of the instrument leading to anomalous wind speed values. Based on comparisons to reanalysis winds, Schmidt et al. (2017) suggested that autonomous platforms like the Minimet measuring winds in challenging conditions characterized by high wind and sea states would likely underestimate true wind speed. Generally, these differences would be expected to manifest as reanalysis wind speed being larger than those measured in situ and affected by wave crest sheltering (Large et al. 1995; Renfrew et al. 2020; Schmidt et al. 2017).

As mentioned previously, the internal preprocessing of the Minimet winds aims to eliminate anomalous wind values due to sheltering effects and instrument submersion. Intercomparisons between Minimet, R/V *Armstrong*, and ERA5 winds interpolated onto the respective drifter and vessel positions revealed ERA5 winds were generally smaller than both R/V *Armstrong* and Minimet winds over a range of wind speeds, and wind speed differences were wind speed dependent. The

observed wind speed differences between Minimets and ERA5 were consistent during both the cruise periods and when the entire observation period was considered. The wind speed differences observed between ERA5 and Minimet winds were hence inconsistent with wind sheltering effects. Similar to the results in this present study, wind-speed-dependent differences between reanalysis winds and buoy measurements were reported by Jones et al. (2016) and Stopa and Cheung (2014), as well as between ship winds and ERA5 (Renfrew et al. 2020).

The validation of Minimet winds against coincident ship winds from R/V *Armstrong* has shown that the Minimets measure winds reliably. Additionally, the fact that wind speed differences between ERA5 and Minimets increased in the presence of larger local gradients in the ERA5 reanalysis model wind fields suggest the observed discrepancies between Minimets and ERA5 are likely due to potential limitations of the latter. While ERA5 reanalysis winds represent a significant improvement overall compared to previous generation ERA reanalysis models (Belmonte Rivas and Stoffelen 2019), our results indicate that Minimet winds better represented true wind speed magnitudes, particularly at superinertial frequencies, than ERA5 during the observation period considered here. These results highlight the fact that verification of gridded wind products through in situ wind measurements, particularly in poorly sampled regions, remains vital.

Despite its hourly resolution, near-inertial and particularly superinertial spectral energy on both sides of the ERA5 rotary wind spectrum was considerably smaller than that estimated from hourly Minimet winds. This is in agreement with results by Liu et al. (2019), who found near-inertial wind power estimates derived from surface drifters in combination with a 6-hourly gridded wind product to be systematically smaller than in situ buoy estimates. The authors concluded these differences were due to reduced near-inertial variance in the wind product and additionally found no significant improvement in their near-inertial wind power estimates when using an hourly reanalysis product. The results from the present study further suggest that, despite their improved hourly resolution, wind variability in the ERA5 reanalysis winds at near-inertial and superinertial frequencies is likely underestimated in and poleward of the study region considered here.

Near-inertial wind power input was estimated using Minimet drifter velocities and coincident in situ sea surface winds measured by Minimet drifters. These were compared to estimates from hourly ERA5 reanalysis winds linearly interpolated onto drifter positions. While both estimates showed a net input of energy into the mixed layer by the wind over the study period, the use of in situ winds measured by Minimet drifters resulted in a 42% higher time-averaged near-inertial wind power input over the observation period relative to that estimated using hourly ERA5 reanalysis winds. The approach taken in this study involved using in situ wind measurements along the track of the Minimet surface drifter and represents the most desirable option to estimate near-inertial wind power input into the mixed layer, obviating the need for modeled mixed layer velocities and gridded wind products.

The importance of high-frequency wind variability for accurate near-inertial wind power estimates was further evidenced by wind events happening on time scales far smaller than the local inertial period that were not captured in the reanalysis model and lead to large discrepancies between wind power estimates from Minimet and ERA5 winds. Plueddemann and Farrar (2006) showed that wind events with the largest contribution to time-averaged near-inertial wind power input occur on time scales much shorter than the local inertial period. We found events lasting less than half the average inertial period in our study contributing significantly to the discrepancies between ERA5 and Minimet-derived near-inertial wind power input estimates. These events comprised about 5% of our dataset. As such, these results imply that high-resolution wind products are necessary to capture small-scale wind events and to adequately resolve near-inertial wind power input. Lower-resolution wind products may fail to accurately represent these short wind events (e.g., Kilbourne and Girton 2015) and hence underestimate wind work. Our results further emphasize the utility of platforms like the Minimet for validating and possibly correcting regional and global estimates from reanalysis products in combination with surface drifter data.

Cospectra of Minimet wind stress and drifter velocities showed significantly increased wind work in the near-inertial band compared to those estimated from Minimet drifter velocities and ERA5 winds. Negative cospectral values estimated from Minimet drifter velocities and both Minimet and ERA5 winds further suggested that the wind effectively acted to remove energy from the mixed layer at superinertial frequencies, reducing overall wind power input in the near-inertial band. The negative wind power at superinertial frequencies coincided with a shoulder at the semidiurnal tidal frequency on the clockwise side of the drifter velocity rotary spectrum (cf. Fig. 6b), suggesting that the wind acting on the semidiurnal tides acts to remove energy from the ocean. As mentioned previously, this peak was larger on the clockwise side compared to the counterclockwise side, pointing to an anticyclonic polarization of the semidiurnal tide (see also Thomson et al. 1998; Poulain and Centurioni 2015). These results are further in agreement with recent results by Flexas et al. (2019), who showed negative superinertial wind power occurring at the semidiurnal tidal frequencies across a range of wavenumbers at several geographical locations in a global ocean model. The exact mechanisms underlying this negative wind power at superinertial frequencies exceed the scope of this paper but certainly warrant further investigation.

The present study aimed to validate in situ wind measurements from the Minimet drifter against coincident ship measurements. Further, in the first study of its kind, it applied these novel wind measurements to the near-inertial wind power problem. Comparisons to ship winds during the two cruise periods indicate that there is a general utility for Minimets to be deployed in regions other than the one highlighted here to reliably measure winds along their drifter track. The results of this study do not, however, permit to make a general statement about discrepancies between ERA5 reanalysis winds and in situ wind measurements, and any potential limitations of the former might be regional.

Wind measurements from Minimet drifters can aid in further investigating the skill of reanalysis model winds and

potential discrepancies with in situ winds, particularly in sparsely sampled or difficult to sample regions. Sustaining a Minimet array over at least one season at a basin scale would lead to an interesting verification, or otherwise, of near-inertial wind power input estimates from reanalysis products and highlight the need for maintaining arrays of Minimets at key locations. Similar to a correction method employed by Liu et al. (2019), who used the ratio of the variances of their wind product and buoy winds averaged over the near-inertial band as a correction factor, a suitable approach in our case would be to follow a method similar to that outlined in Elipot (2006) and Elipot and Gille (2009b). The ratio of ERA5- and Minimet-estimated cospectra could provide a frequency-dependent correction for the ERA5-estimated near-inertial wind power input and provide a measure of uncertainty in the near-inertial range. This could be a way to utilize high-resolution in situ wind measurements from Minimet drifters to estimate the degree to which reanalysis products under- or overestimate near-inertial wind power input and apply corrections when necessary. This approach would require a lot more data, but regional deployments could aid in quantifying the error associated with using gridded wind products and hence improve our estimates of near-inertial wind power input globally, important for accurately depicting abyssal mixing in general circulation and climate models.

Acknowledgments. T. Klenz and H. L. Simmons were supported by NSF Grant 1658302 and ONR Grant N000141812386. L. Centurioni and V. Hormann were supported by ONR Grant N000141812445. J. M. Lilly and J. J. Early were supported by NSF Grant 1658564. Minimet drifters used in this study were funded by ONR Grant N000141712517 and NOAA Grant NA150AR4320071 "The Global Drifter Program." We thank the captain and crew of the R/V *Neil Armstrong*. Drifter velocities and spectral estimates were calculated using co-author J. M. Lilly's MATLAB toolbox, jLab (Lilly 2021). The authors are grateful to Mark Inall and an anonymous reviewer for their comments and suggestions during the review process, which led to an improved paper.

Data availability statement. European Centre for Medium-Range Weather Forecasts ERA5 reanalysis wind data used during this study are openly available from the Research Data Archive at the National Center for Atmospheric Research, Computational and Information Systems Laboratory at https://doi.org/10.5065/BH6N-5N20. All shipboard and drifter data collected as part of the U.S. Office of Naval Research Near-Inertial Shear and Kinetic Energy in the North Atlantic experiment (NISKINe) is still in the process of being organized and archived. All data will be fully released to the public when the program formally concludes. NISKINe data presented in this study are available from the corresponding author upon reasonable request.

REFERENCES

Alford, M. H., 2001: Internal swell generation: The spatial distribution of energy flux from the wind to mixed layer near-inertial motions. *J. Phys. Oceanogr.*, **31**, 2359–2368, https://doi.org/10.1175/1520-0485(2001)031<2359:ISGTSD>2.0.CO;2.

——, 2003a: Improved global maps 54-year history of wind-work on ocean inertial motions. *Geophys. Res. Lett.*, **30**, 1424, https://doi.org/10.1029/2002GL016614.

——, 2003b: Redistribution of energy available for ocean mixing by long-range propagation of internal waves. *Nature*, **423**, 159–163, https://doi.org/10.1038/nature01628.

——, 2020: Revisiting near-inertial wind work: Slab models, relative stress and mixed-layer deepening. *J. Phys. Oceanogr.*, **50**, 3141–3156, https://doi.org/10.1175/JPO-D-20-0105.1.

Belmonte Rivas, M., and A. Stoffelen, 2019: Characterizing ERA-Interim and ERA5 surface wind biases using ASCAT. *Ocean Sci.*, **15**, 831–852, https://doi.org/10.5194/os-15-831-2019.

Centurioni, L., A. Horányi, C. Cardinali, E. Charpentier, and R. Lumpkin, 2017: A global ocean observing system for measuring sea level atmospheric pressure: Effects and impacts on numerical weather prediction. *Bull. Amer. Meteor. Soc.*, **98**, 231–238, https://doi.org/10.1175/BAMS-D-15-00080.1.

Centurioni, L. R., 2018: *Drifter Technology and Impacts for Sea Surface Temperature, Sea-Level Pressure, and Ocean Circulation Studies.* Springer International Publishing, 37–57, https://doi.org/10.1007/978-3-319-66493-4_3.

D'Asaro, E. A., 1985: The energy flux from the wind to near-inertial motions in the surface mixed layer. *J. Phys. Oceanogr.*, **15**, 1043–1059, https://doi.org/10.1175/1520-0485(1985)015<1043:TEFFTW>2.0.CO;2.

ECMWF, 2019: ERA5 reanalysis (0.25 degree latitude-longitude grid). Research Data Archive at the National Center for Atmospheric Research, Computational and Information Systems Laboratory, accessed 24 February 2020, https://doi.org/10.5065/BH6N-5N20.

Elipot, S., 2006: Spectral characterization of Ekman velocities in the Southern Ocean based on surface drifter trajectories. Ph.D. thesis, University of California, San Diego, 126 pp., https://escholarship.org/uc/item/1ks7v6wm.

——, and S. T. Gille, 2009a: Ekman layers in the Southern Ocean: Spectral models and observations, vertical viscosity and boundary layer depth. *Ocean Sci.*, **5**, 115–139, https://doi.org/10.5194/os-5-115-2009.

——, and ——, 2009b: Estimates of wind energy input to the Ekman layer in the Southern Ocean from surface drifter data. *J. Geophys. Res.*, **114**, C06003, https://doi.org/10.1029/2008JC005170.

——, R. Lumpkin, R. C. Perez, J. M. Lilly, J. J. Early, and A. M. Sykulski, 2016: A global surface drifter data set at hourly resolution. *J. Geophys. Res. Oceans*, **121**, 2937–2966, https://doi.org/10.1002/2016JC011716.

Emery, W., and R. Thomson, 2001: *Data Analysis Methods in Physical Oceanography.* Elsevier, 729 pp.

Flexas, M. M., A. F. Thompson, H. S. Torres, P. Klein, J. T. Farrar, H. Zhang, and D. Menemenlis, 2019: Global estimates of the energy transfer from the wind to the ocean, with emphasis on near-inertial oscillations. *J. Geophys. Res. Oceans*, **124**, 5723–5746, https://doi.org/10.1029/2018JC014453.

Gille, S. T., 2005: Statistical characterization of zonal and meridional ocean wind stress. *J. Atmos. Oceanic Technol.*, **22**, 1353–1372, https://doi.org/10.1175/JTECH1789.1.

Goni, G. J., and Coauthors, 2017: Autonomous and Lagrangian ocean observations for Atlantic tropical cyclone studies and forecasts. *Oceanography*, **30**, 92–103, https://doi.org/10.5670/oceanog.2017.227.

Hansen, D. V., and P.-M. Poulain, 1996: Quality control and interpolations of WOCE-TOGA drifter data. *J. Atmos. Oceanic Technol.*, **13**, 900–909, https://doi.org/10.1175/1520-0426(1996)013<0900:QCAIOW>2.0.CO;2.

Hormann, V., L. R. Centurioni, L. Rainville, C. M. Lee, and L. J. Braasch, 2014: Response of upper ocean currents to Typhoon Fanapi. *Geophys. Res. Lett.*, **41**, 3995–4003, https://doi.org/10.1002/2014GL060317.

Jayne, S. R., and L. C. St. Laurent, 2001: Parameterizing tidal dissipation over rough topography. *Geophys. Res. Lett.*, **28**, 811–814, https://doi.org/10.1029/2000GL012044.

Jones, R. W., I. A. Renfrew, A. Orr, B. G. Webber, D. M. Holland, and M. A. Lazzara, 2016: Evaluation of four global reanalysis products using in situ observations in the Amundsen Sea embayment, Antarctica. *J. Geophys. Res. Atmos.*, **121**, 6240–6257, https://doi.org/10.1002/2015JD024680.

Kilbourne, B. F., and J. B. Girton, 2015: Quantifying high-frequency wind energy flux into near-inertial motions in the southeast Pacific. *J. Phys. Oceanogr.*, **45**, 369–386, https://doi.org/10.1175/JPO-D-14-0076.1.

Landwehr, S., I. Thurnherr, N. Cassar, M. Gysel-Beer, and J. Schmale, 2020: Using global reanalysis data to quantify and correct airflow distortion bias in shipborne wind speed measurements. *Atmos. Meas. Tech.*, **13**, 3487–3506, https://doi.org/10.5194/amt-13-3487-2020.

Large, W. G., and S. Pond, 1981: Open ocean momentum flux measurements in moderate to strong winds. *J. Phys. Oceanogr.*, **11**, 324–336, https://doi.org/10.1175/1520-0485(1981)011<0324:OOMFMI>2.0.CO;2.

——, J. Morzel, and G. B. Crawford, 1995: Accounting for surface wave distortion of the marine wind profile in low-level Ocean Storms wind measurements. *J. Phys. Oceanogr.*, **25**, 2959–2971, https://doi.org/10.1175/1520-0485(1995)025<2959:AFSWDO>2.0.CO;2.

Lilly, J. M., 2017: Element analysis: A wavelet-based method for analysing time-localized events in noisy time series. *Proc. Roy. Soc.*, **473**, 1–28, https://doi.org/10.1098/rspa.2016.0776.

——, 2021: jlab: A data analysis package for Matlab, v. 1.7.0. http://www.jmlilly.net/software.

——, and S. Elipot, 2021: A unifying perspective on transfer function solutions to the unsteady Ekman problem. *Fluids*, **6**, 2311–5521, https://doi.org/10.3390/fluids6020085.

Liu, Y., Z. Jing, and L. Wu, 2019: Wind power on oceanic near-inertial oscillations in the global ocean estimated from surface drifters. *Geophys. Res. Lett.*, **46**, 2647–2653, https://doi.org/10.1029/2018GL081712.

Lumpkin, R., and M. Pazos, 2007: Measuring surface currents with surface velocity program drifters: The instrument, its data, and some recent results. *Lagrangian Analysis and Prediction in Coastal and Ocean Processes*, A. Griffa et al., Eds., Cambridge University Press, 39–67, https://doi.org/10.1017/CBO9780511535901.003.

——, L. Centurioni, and R. C. Perez, 2016: Full access fulfilling observing system implementation requirements with the global drifter array. *J. Atmos. Oceanic Technol.*, **33**, 685–695, https://doi.org/10.1175/JTECH-D-15-0255.1.

Maximenko, N., R. Lumpkin, and L. Centurioni, 2013: Ocean surface circulation. *Ocean Circulation and Climate: A 21st Century Perspective*, International Geophysics Series, Vol. 103, Academic Press, 283–304, https://doi.org/10.1016/B978-0-12-391851-2.00012-X.

Munk, W., and C. Wunsch, 1998: Abyssal recipes II: Energetics of tidal and wind mixing. *Deep-Sea Res. I*, **45**, 1977–2010, https://doi.org/10.1016/S0967-0637(98)00070-3.

Niiler, P., 2001: The world ocean surface circulation. *Ocean Circulation and Climate: Observing and Modelling the Global Ocean*, International Geophysics Series, Vol. 77, Academic Press, 193–204, https://doi.org/10.1016/S0074-6142(01)80119-4.

——, A. S. Sybrandy, K. Bi, P. M. Poulain, and D. Bitterman, 1995: Measurements of the water-following capability of holey-sock and TRISTAR drifters. *Deep-Sea Res. I*, **42**, 1951–1964, https://doi.org/10.1016/0967-0637(95)00076-3.

Plueddemann, A. J., and J. T. Farrar, 2006: Observations and models of the energy flux from the wind to mixed-layer inertial currents. *Deep-Sea Res. II*, **53**, 5–30, https://doi.org/10.1016/j.dsr2.2005.10.017.

Pollard, R. T., and R. C. Millard, 1970: Comparison between observed and simulated wind-generated inertial oscillations. *Deep-Sea Res. Oceanogr. Abstr.*, **17**, 813–821, https://doi.org/10.1016/0011-7471(70)90043-4.

Poulain, P. M., and L. Centurioni, 2015: Direct measurements of World Ocean tidal currents with surface drifters. *J. Geophys. Res. Oceans*, **120**, 6986–7003, https://doi.org/10.1002/2015JC010818.

Price, J. F., R. A. Weller, and R. Pinkel, 1986: Diurnal cycling: Observations and models of the upper ocean response to diurnal heating, cooling, and wind mixing. *J. Geophys. Res.*, **91**, 8411–8427, https://doi.org/10.1029/JC091iC07p08411.

Rath, W., R. J. Greatbatch, and X. Zhai, 2013: Reduction of near-inertial energy through the dependence of wind stress on the ocean-surface velocity. *J. Geophys. Res. Oceans*, **118**, 2761–2773, https://doi.org/10.1002/jgrc.20198.

Renfrew, I. A., and Coauthors, 2020: An evaluation of surface meteorology and fluxes over the Iceland and Greenland Seas in ERA5 reanalysis: The impact of sea ice distribution. *Quart. J. Roy. Meteor. Soc.*, **147**, 691–712, https://doi.org/10.1002/qj.3941.

Schmidt, K. M., S. Swart, C. Reason, and S. A. Nicholson, 2017: Evaluation of satellite and reanalysis wind products with in situ wave glider wind observations in the Southern Ocean. *J. Atmos. Oceanic Technol.*, **34**, 2551–2568, https://doi.org/10.1175/JTECH-D-17-0079.1.

Simmons, H. L., and M. H. Alford, 2012: Simulating the long-range swell of internal waves generated by ocean storms. *Oceanography*, **25**, 30–41, https://doi.org/10.5670/oceanog.2012.39.

Slepian, D., 1978: Prolate spheroidal wave functions, Fourier analysis, and uncertainty—V: The discrete case. *Bell Syst. Tech. J.*, **57**, 1371–1430, https://doi.org/10.1002/j.1538-7305.1978.tb02104.x.

Smith, S. R., M. A. Bourassa, and R. J. Sharp, 1999: Establishing more truth in true winds. *J. Atmos. Oceanic Technol.*, **16**, 939–952, https://doi.org/10.1175/1520-0426(1999)016<0939:EMTITW>2.0.CO;2.

St. Laurent, L., and H. Simmons, 2006: Estimates of power consumed by mixing in the ocean interior. *J. Climate*, **19**, 4877–4890, https://doi.org/10.1175/JCLI3887.1.

Stopa, J. E., and K. F. Cheung, 2014: Intercomparison of wind and wave data from the ECMWF reanalysis interim and the NCEP climate forecast system reanalysis. *Ocean Modell.*, **75**, 65–83, https://doi.org/10.1016/j.ocemod.2013.12.006.

Thomson, R. E., P. H. Leblond, and A. B. Rabinovich, 1998: Satellite-tracked drifter measurement of inertial and semidiurnal currents in the northeast Pacific. *J. Geophys. Res.*, **103**, 1039–1052, https://doi.org/10.1029/97JC02374.